A New Strategy for Infrastructural Health Monitoring Using Radar Remote Sensing

Guoqiang Shi[1], Hui Lin[1,2], Peifeng Ma[1], Yuzhou Liu[1]

1: Institute of Space and Earth Information Science, The Chinese University of Hong Kong
2: Shenzhen Research Institute, The Chinese University of Hong Kong

ABSTRACT:
On the expectation of performing better infrastructural health monitoring in urban and semi-artificial regions, we intend to achieve better integrity of deformation mapping with the detection of homogeneous objects. To monitor the semi-artificial regions (e.g., pavements and small grassed lands) that are normally distributed scatterers (DSs) in SAR images, homogeneous pixels will be analyzed on the basis of tomography SAR. Two layers are designed for the networking of PS and DS candidates. In the first-tier network, we detect the most reliable PSs as the reference points in the follow-up processing, and connect them using a Delaunay triangulation network. In the second-tier network, homogeneous pixels are clustered for the detection of potential DS candidates by performing an adaptive homogeneous filter. Geophysical parameters (e.g., deformation velocity) of DS candidates are estimated using the Capon beam-forming algorithm. Preliminary result from 40 C-band Sentinel-1A scenes of the Hong Kong International Airport is given in this paper.

Keywords: Health monitoring, Persistent Scatterers (PSs), Distributed Scatterers (DSs), Adaptive Homogeneous Filter.

INTRODUCTION

The emergence of numerous new infrastructures, attributed to the constant promotion of urbanization, has increased the possibility of hidden "Urban Disease" related to structural safety. Being short of regular infrastructural health monitoring, e.g., detection of abnormal structural deformation, the maintenance of those infrastructures (e.g., airports, highways, railways, buildings, bridges, dams, tunnels, etc.) is usually not well coordinated. Typically, these structural deformation and surface subsidence are mainly caused by natural (e.g., wind, soil dissolution, etc.) and/or human forces (e.g., groundwater extraction, underground constructions, etc.), which will become even trickier with the accelerating urbanization. These potential risks could somehow threaten our public life and property safety. Owing to the characteristics of radar remote sensing, interferometric synthetic aperture radar (InSAR) has its unique capability of monitoring spatially large-scale and temporally long-term movements of land surface, which provides an efficient solution for health monitoring of built territory [1-4]. The persistent scatterers interferometry (PSI) method, as a classical multi-temporal method, is able to obtain submeter accuracy digital elevation model (DEM) and theoretically millimeter level accuracy in surface motion detection [3]. PSI holds its good performance in regions with high reflectivity and stable targets, e.g., buildings [2,3]. To improve its capability in today's complex urban environment, the more recent Tomo-PSInSAR integrates conventional PSI with multi-dimensional SAR tomography to properly solve the overlaid problem [1,5]. This technique provides full 3-D imaging of layover and semitransparent regions [1,4,5], e.g., heavy built urban areas, multilayer structures, etc., which presents us with more detailed structural deformations of the city jungle. These, certainly guarantee the implementation of urban safety monitoring.

However, the point-wise scatterers are hardly to be detected on low correlation areas [2,6] (e.g., the low reflectivity airport pavements), of which the limitation may cause missing detection of abnormal motion patterns due to insufficient scatterers. To this end, we propose a new strategy for infrastructural health monitoring on these regions based on the combined analysis of persistent and distributed scatterers. Basically, the jointly detection of PS and DS is accomplished by exploiting a two-tier network strategy through which the atmospheric phase screen (APS) can be removed. The most reliable PS points are firstly detected in the first-tier network and are used as references points for the extended PS and DS in the follow-up processing. In the second-tier network, we perform an adaptive homogeneous filter to identify statistically homogeneous pixels (SHPs) and select possible DS candidates to build up the DS network.

After removing the atmospheric delay by subtracting the phase of nearest reference points, the geophysical parameters of DS points are directly estimated using Capon beam-forming algorithm. A preliminary result of the HK international airport is given using 40 Sentinel-1A data.

METHODOLOGY

Basically, our strategy can be divided into two parts, namely, the PS network and DS network, as given in Fig.1.

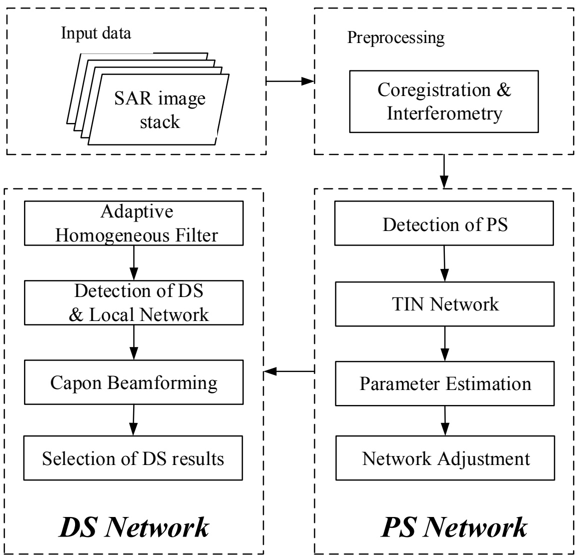

Fig. 1. Flowchart of the proposed method

• *PS network*

In the PS network, the object is to detect the most reliable/high-quality PS candidates as we are going to set our reference network based on those scatterers. Meanwhile, the precision of the parameter estimates on the first-tier PS points should be highly guaranteed. The amplitude dispersion index (ADI) in (1), where σ_A and E_A are the standard deviation and the mean value of the data vector's amplitude, respectively, is used for the initial selection of the PS candidates. The network is then established by connecting those reference PS points using a Delaunay triangulation network.

$$ADI = \frac{\sigma_A}{E_A} \quad (1)$$

The atmospheric delay on one of the two PSs can be removed by subtracting the phase of its adjacent PS point. In order to increase the spatial density of available ground observations, we extend the PS network by detecting all the remaining PSs according to the temporally averaged amplitude, i.e., E_A. After excluding the reference PS points detected above, pixels with $E_A > E_T$ are selected as potential candidates. The selection of E_T is usually depending on the capability of separating built environments and low correlation territories, e.g., water, shadows. These new PS pixels are then linked to their nearest reference points, building up local star networks. We estimate the parameters on the reference PS points through a combined use of beam-forming and M-estimator [1]. Parameters of PS candidates can be estimated by solving the tomography [1]

$$\hat{\gamma}(s,v) = \frac{|a(s,v)^H y|}{\|a(s,v)^H\|_2 \|y\|_2} \quad (2)$$

where $\hat{\gamma}$ is the estimated tomography, y is the complex data vector, $\|\cdot\|_2$ is the 2-norm calculation factor. a is the steering vector

$$a(s,v) = \begin{bmatrix} \exp\,(j2\pi(\xi_1 s + \eta_1 v)) \\ \vdots \\ \exp\,(j2\pi(\xi_N s + \eta_N v)) \end{bmatrix} \quad (3)$$

where s and v represent the elevation and linear motion velocity to be estimated, respectively. ξ_N is the spatial frequency and η_N the temporal frequency.

• *DS network*

As stated in [2], the spatial filter used for DS detection should be able to average the statistically homogeneous pixels only. Considering the textural features of the semi-artificial regions and on the expectation of reducing false alarms in homogeneity test, we perform the homogeneous pixels clustering by the combination of a direction-based window and the Anderson-Darling (AD) test [7,8], namely the adaptive homogeneous filter. In this work, we design a circular window with 18 directions of the inner sub-window. The identification of a proper direction of the sub-window, i.e., w_θ, is based on the lowest variance among all the tested directions.

$$w_\theta = arg\,\min_\theta \left(var\left(\bar{x}(w_\theta)\right)\right), \theta = 0°, 10°, \cdots, 170° \quad (4)$$

where $\bar{x}$ is the temporal mean of amplitude value. By selecting a proper candidate window, within which the featureless areas are captured, the probability of miscollection of inhomogeneous neighbors can be reduced. The two-sample AD test is then applied within the determined window for SHP clustering. We perform the test under a significance level of 5% and use the identified SHP families for despeckle filtering. Fig.2 gives the filtered amplitude images of the Hong Kong International Airport (HKIA) from sentinel-1 A data.

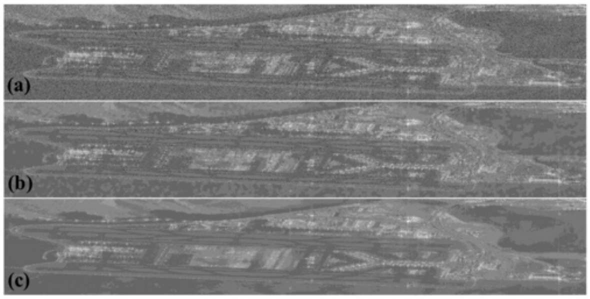

Fig.2 Amplitude images of HKIA from (a) original, (b) homogeneous filter with box window and (c) the adaptive homogeneous filter.

Detected DSs are then connected to the PS reference network, geophysical parameters of DS are obtained by solving the Capon power [9]

$$\tilde{\sigma}_0^2 = \frac{1}{A^H \hat{R}^{-1} A} \tag{5}$$

where $(.)^H$ donates conjugate transpose, A is the steering matrix which is composed of a. $\hat{R}$ is the estimated covariance matrix of the data vector. In order to make the estimation more robust, a loading factor can be added into the covariance matrix [9]. Fig.3 shows the normalized estimated $\hat{R}$ based on normal box window and the selected SHPs. Due to the clustering of homogeneous scatterers, the coherence of DS candidate is improved compared with simple multi-looking of all pixels within the box window.

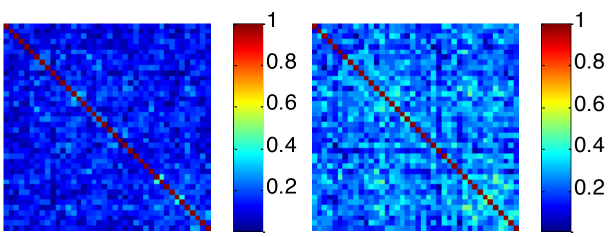

Fig.3 Coherence matrix estimated from (left) box window and (right) the SHPs family.

EXPERIMENTAL RESULT

The Hong Kong international airport was built on reclaimed lands due to the space limitation in Hong Kong. Being one of the largest reclaimed areas in the world, 75% of the airport was reclaimed from the sea. Consequently, the ground and facilities constructed on it may be subject to settlement caused by unconsolidated subsurface soil layers and penetration of seawater. In this work, 40 Sentinel-1 A images observed from 15-06-2015 to 28-02-2017 are used for the experiment. We choose the acquisition obtained on 22-04-2016 as our master scene, interferometry is conducted with single-look pixels. Our study area is given in Fig.4.

Fig.4 The Hong Kong International Airport (HKIA) visualized in google earth.

According to Fig.5 (a), the PS network only gives the general outline of the airport and mainly covers the stereoscopic structures, e.g., the terminal buildings. Those areas with weak radar returns such as pavements and bare soil (middle of the airport, Fig.4) contain very limited PS candidates owing to their low correlation of the data stack. The missing detection of sufficient measurement points may lose structure details especially on the pavements, which is one of the most important considerations for airport safety monitoring. By introducing the distributed scatterers, our result in Fig.5 (b) has shown a great improvement in reflecting structural details and the point density. Deformation of those missing regions is successfully recovered, making the airport pavements and other low correlation parts clearly presented in the monitoring map.

The airport was reclaimed based on the two original rocky islands of Chek Lap Kok and Lam Chau, marked as red polygons in Fig.5. Other than the two islands which are relatively stable, the remaining lands are subject to uneven subsidence with a maximum rate of approximately 20 mm/year. Compared with PS result, this integrated strategy can help to easily locate critical settlement zones, for example the north pavement and the middle construction areas. Therefore, better decision making on distress tracking and follow-up monitoring.

SUMMARY

In this work, we introduce the strategy of combining PS and DS processing to conduct more robust deformation estimation and thus better integrity of safety monitoring over semi-artificial places. The adaptive homogeneous filter is used for the clustering of statistically homogeneous pixels. We set up the two-tier hierarchical network for the connecting of PS and DS candidates using Delaunay triangulation and local networks. Parameters of the detected PS and DS are solved using robust estimators, e.g., M-estimator, Capon beam-forming. Results from 40 sentinel-1data of the HK airport are given. The proposed method has greatly improved the performance of deformation detection by enhancing useful radar returns on low correlation areas. Further studies will be carried out on the improvement of computational efficiency of parameter estimation and the optimization of coherence matrix.

ACKNOWLEDGEMENT

The authors would like to thank the European space agency (ESA) for providing the Sentinel-1 A data.

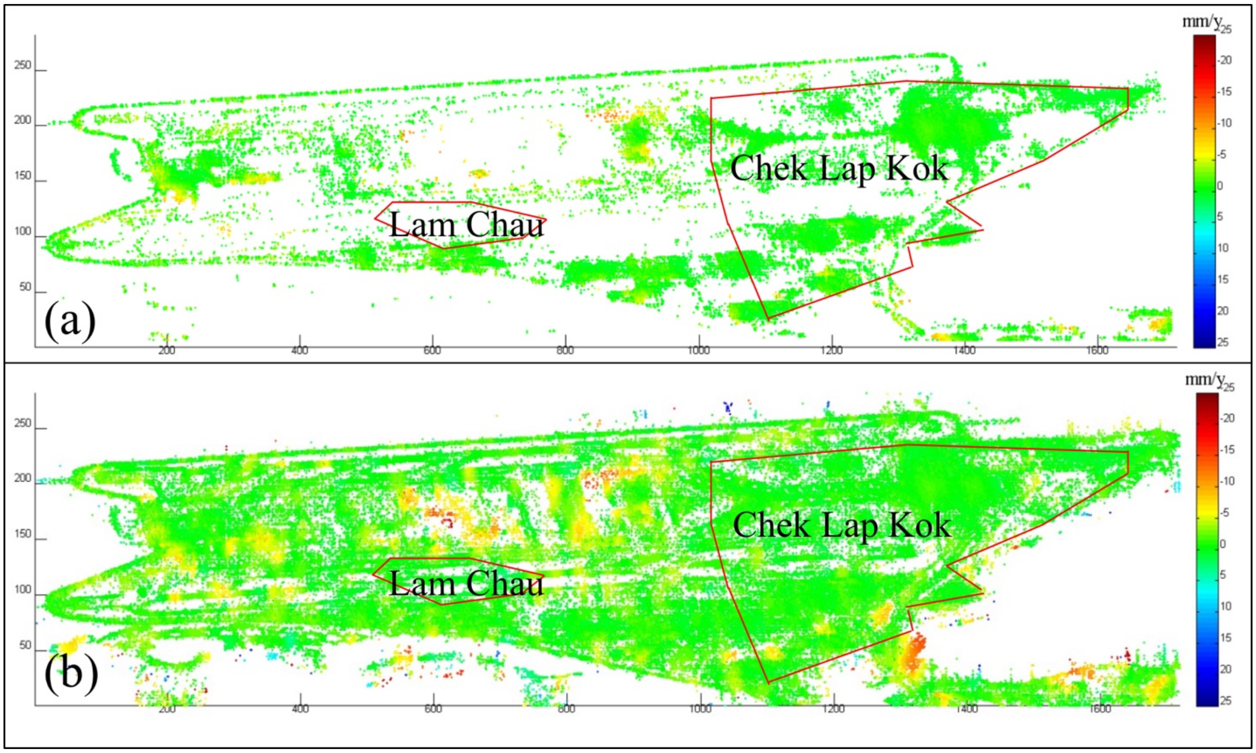

Fig.5 Linear deformation map of the Hong Kong Airport from (a) PS only and (b) the proposed method, both are displayed in radar coordinate with full resolution. Color red and green indicate subsidence and stable regions, respectively.

REFERENCES

[1] P. Ma, H. Lin, "Robust Detection of Single and Double Persistent Scatterers in Urban Built Environments," *Geoscience and Remote Sensing, IEEE Transactions on* PP, 1 (2015).

[2] A. Ferretti et al., "A New Algorithm for Processing Interferometric Data-Stacks: SqueeSAR," *Geoscience and Remote Sensing, IEEE Transactions on* 49, 3460 (2011).

[3] Ferretti, A, C. Prati, and F. Rocca. "Permanent scatterers in SAR interferometry." *Geoscience & Remote Sensing, IEEE Transactions on* 39.1(2001):8-20.

[4] X. X. Zhu, R. Bamler, "Let's Do the Time Warp: Multicomponent Nonlinear Motion Estimation in Differential SAR Tomography," *Geoscience and Remote Sensing Letters, IEEE* 8, 735 (2011).

[5] F. Lombardini, "Differential tomography: a new framework for SAR interferometry," *Geoscience and Remote Sensing, IEEE Transactions on* 43, 37 (Jan., 2005).

[6] Jiang, Mi, X. Ding, and R. Hanssen. "Deformation Monitoring over Low Coherence Area Using Multisource DS-InSAR Technique." *Dragon 3Mid Term Results*, 2014.

[7] Parizzi, Alessandro, and R. Brcic. "Adaptive InSAR Stack Multilooking Exploiting Amplitude Statistics: A Comparison Between Different Techniques and Practical Results." *IEEE Geoscience & Remote Sensing Letters* 8.3(2011):441-445.

[8] Wang, Yuanyuan, X. X. Zhu, and R. Bamler. "Retrieval of phase history parameters from distributed scatterers in urban areas using very high resolution SAR data." *Isprs Journal of Photogrammetry & Remote Sensing* 73.9(2012):89-99.

[9] Lombardini, F, and A. Reigber. "Adaptive spectral estimation for multibaseline SAR tomography with airborne L-band data." *Geoscience and Remote Sensing Symposium, 2003. IGARSS '03. Proceedings. 2003 IEEE International IEEE*, 2003:2014-2016.